# THE CO DISTRIBUTION AROUND l=30°, b=0°

by

ALEXANDER SZABO

B. Sc., The University of British Columbia, 1976

A THESIS SUBMITTED IN PARTIAL FULFILLMENT OF

THE REQUIREMENTS FOR THE DEGREE OF

MASTER OF SCIENCE

in

THE FACULTY OF GRADUATE STUDIES

DEPARTMENT OF PHYSICS

We accept this thesis as conforming

to the required standard

THE UNIVERSITY OF BRITISH COLUMBIA

March, 1980

In presenting this thesis in partial fulfilment of the requirements for an advanced degree at the University of British Columbia, I agree that the Library shall make it freely available for reference and study. I further agree that permission for extensive copying of this thesis for scholarly purposes may be granted by the Head of my Department or by his representatives. It is understood that copying or publication of this thesis for financial gain shall not be allowed without my written permission.

Department of Physics

The University of British Columbia
2075 Wesbrook Place
Vancouver, Canada
V6T 1W5

Date March 20, 1980

## Abstract

The 4.6m millimeter wave telescope at the University of British Columbia has been used to map a region 1/2° in diameter centered on l=30°, b=0° in the J=1->0 transition of $^{12}C^{16}O$. This study of the inner edge of the galactic molecular ring has revealed two well defined giant molecular clouds with diameters of approximately 30 pc and masses in the order of 5 x $10^5$ $M_\odot$. In addition our analysis indicates that a substantial fraction, amounting to approximately 30%, of the integrated CO intensity comes from a feature covering the entire field observed. We have also found a complex of four clouds whose linewidths are a factor of two greater than those of the standard giant molecular clouds. The nature of these clouds is at present uncertain. The number of clouds detected in our survey gives as 5000 the total number of giant molecular clouds in the galaxy.

Supervisor: Dr. W.L.H. Shuter

# Table of Contents

page

# List of Tables

page

# List of Figures

page

## Acknowledgements

I thank my thesis supervisor, Dr. W.L.H. Shuter, for his availability, suggestions and encouragement over the last two years.

I thank the other members of the millimeter astronomy group: Dr. W.H. McCutcheon and Mr. C. Chan for their contribution to this project.

Finally, I thank the Computing Center for their help with the numerical calculations.

# 1. INTRODUCTION

Until recently astronomers studying the large scale structure of the galaxy were limited to the detection of radio waves from interstellar hydrogen atoms at a wavelength of 21 cm. Improvements in receiver technology have made it possible to complement this work with studies of the distribution of molecular material in the galaxy by the detection of radio waves from interstellar carbon monoxide (CO) molecules at a wavelength of 2.6 mm.

Previous studies of CO in the galactic plane (Gordon and Burton 1979) have determined that the molecular component of the interstellar gas forms a vast ring of cold star-forming clouds. These studies were limited in that they were under sampled (beam positions spaced at intervals larger than the beam width) and the surveys were one dimensional (beam positions at $l=l_0 + n\Delta l$, $b=0^o$) and thus information on individual clouds was inferred with some difficulty. In order to obtain better information on the nature and size distribution of individual clouds, a well sampled survey in a two dimensional grid is necessary. The study presented here represents one of the first attempts to do this. Figure 1 shows the location of our survey on a depiction of the Galaxy. We decided to center our survey at $l=30^o$, $b=0^o$ because this was an area of especially strong CO emission.

In chapter 2, Data Acquisition, we discuss the methods used to obtain the data. This should prove useful to others involved in millimeter mapping projects. In chapter 3, Data Analysis, we present the data and our interpretation of its significance. The main points are summarised in the Conclusion (chapter 4).

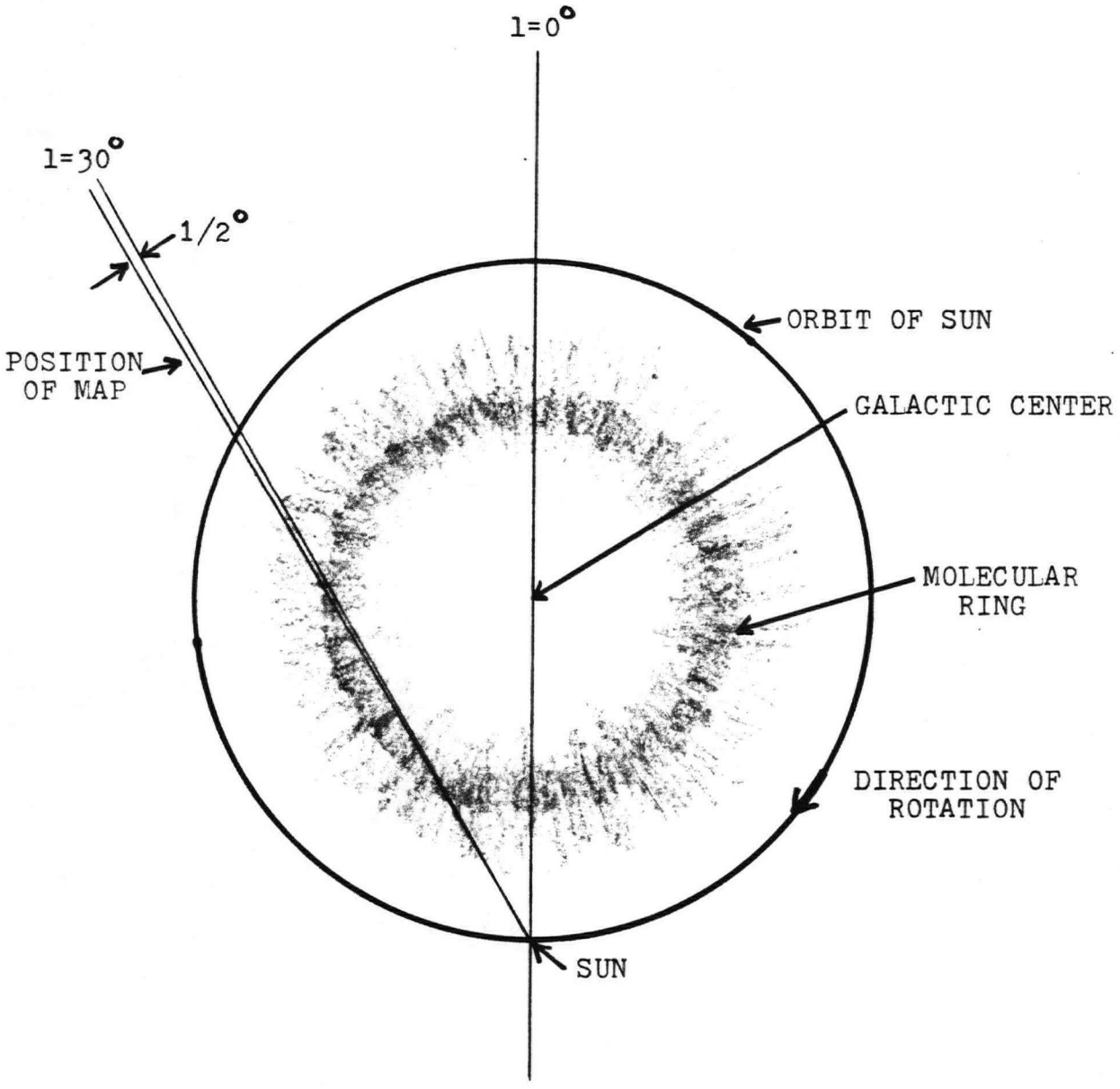


FIGURE 1 : View of the Milky-way galaxy from the north galactic pole showing the molecular ring and the location of our survey in the galactic plane. The molecular ring is believed to have its maximum density just outside the tangential point at l=30°.

## 2. DATA ACQUISITION

### 2.1 Equipment

The observations of l=30°, b=0° which we describe here were obtained using the 4.6m millimeter wave telescope at the University of British Columbia (Shuter and McCutcheon 1974, Mahoney 1976). The telescope is located at latitude 49° 15' 11" N, longitude 123° 13' 56" W, at an elevation of 50 meters. At 115 GHz the paraboloid has an effective beam width of 0.04 degrees which compares with the telescope pointing accuracy of ±0.02 degrees.

Figure 2 shows a schematic diagram of the receiver. At 115 GHz the system noise temperature was 900 kelvin (SSB). The spectra were obtained using a 112 channel filter spectrometer. Each channel was one MHz wide. The spectrometer degraded the theoretical noise figure by a factor of 2.5. The spectra were manipulated, after integration in a digital signal averager, by a NOVA 1200 minicomputer.

FIGURE 2 : Schematic diagram of the UBC 80-120 GHz cooled receiver

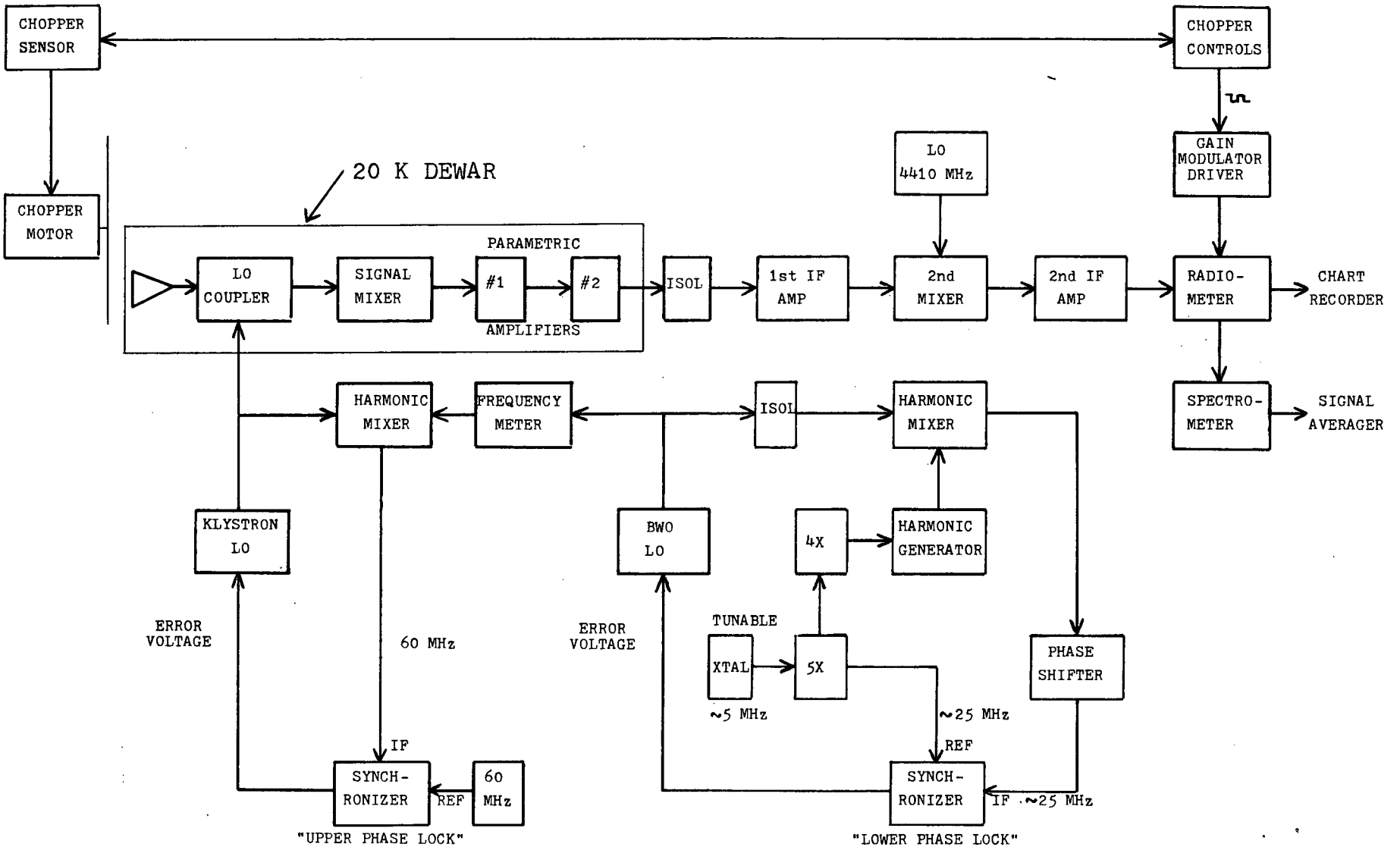

## 2.2 Observing Sequence

Figure 3 shows the beam positions in our survey as they would appear on the sky. The spacing between adjacent beam positions is 0.05 degrees. The 89 beam positions in our map fall inside an area the size of the Moon (as seen from the Earth). For convienence the beam positions were divided into four groups (quarters) and different observing methods were used to obtain the spectra in each group.

The spectra for the first quarter were obtained by alternating between ON source (S) 'scans' and OFF source (R) or reference 'scans'. The term scan used in this paper refers to obtaining a spectrum by integrating on a single fixed beam position. Unless otherwise noted scan integration times were 320 seconds. The purpose of obtaining reference scans is to subtract out the contribution of the sky to the spectra. Each spectrum in the first quarter was the sum of four consecutive ON source minus OFF source pairs. We will represent this as follows


Each night spectra were obtained at five map positions one of which was always the center position. The common spectrum was used to check the accuracy of our relative calibration.

Since one third of the observing time is spent moving the telescope from one map position to another and of the remaining time one half is spent on the OFF source position it was felt that the mapping efficiency could be improved by adopting a different observing sequence. For the second quarter scan

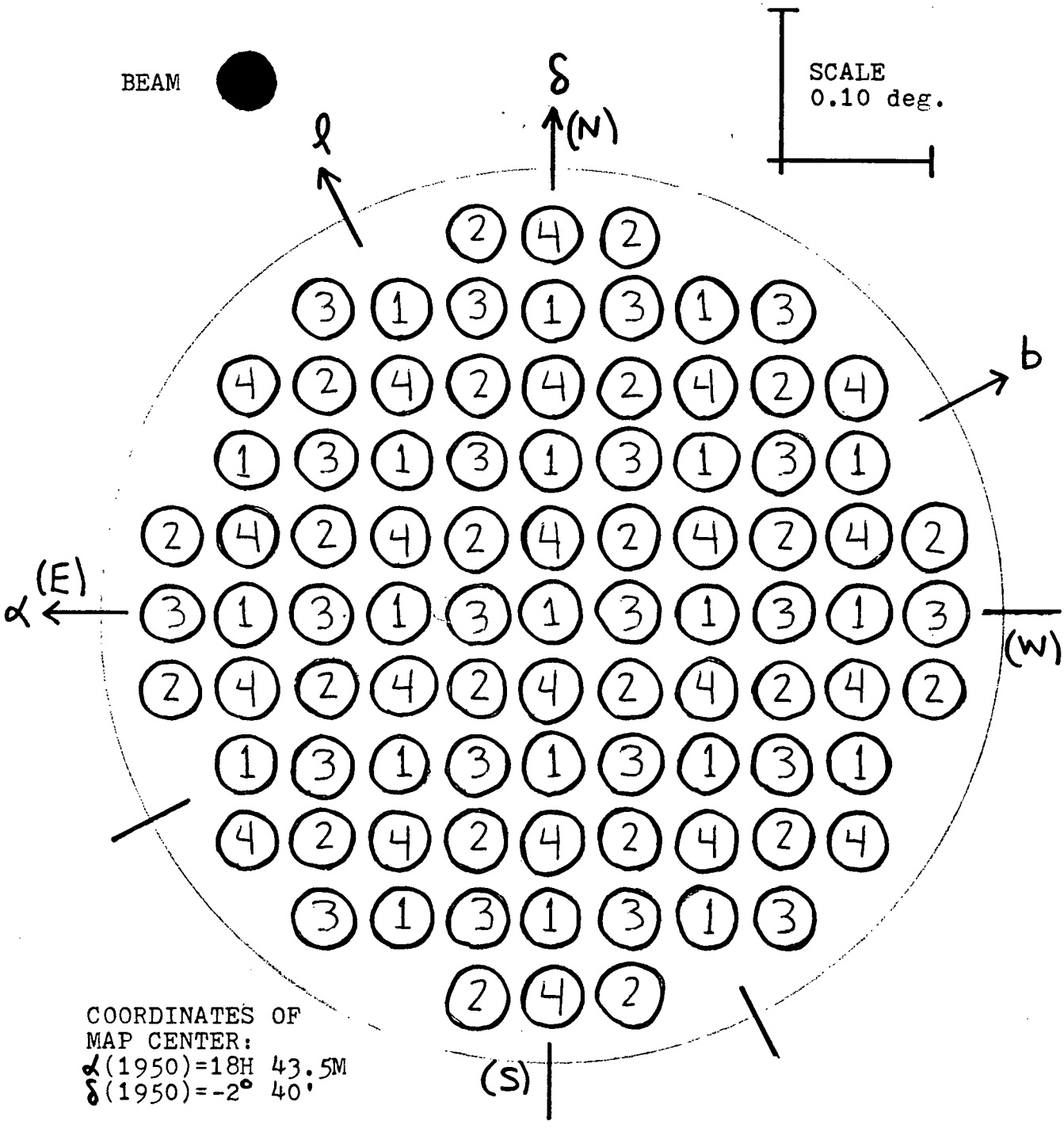


FIGURE 3 : Diagram of the beam positions observed. The map beam positions have been divided into four groups labeled 1, 2, 3, 4.

integration times were increased to 640 seconds to cut in half the number of telescope moves. Also the scans were obtained in such a way that one OFF source scan could be shared by two ON source scans, thus cutting in half the number of reference scans. How this was achieved can best be illustrated as follows

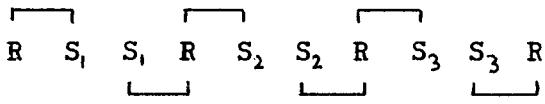


where $S_1$, $S_2$, $S_3$, ... are different beam positions. Beam positions using the same R were relatively far apart to minimize the correlated noise introduced by smoothing (explained later). Notice that telescope moves are also saved because adjacent ON source positions are the same. The net affect was that we could now spend twice as much time ON source per night than before.

This improvement was not however without a price. On some nights the sky would change rapidly enough to make sky correction difficult with long scan times. Thus spectrum baselines were in general worse than before with short scans. Also it was discovered that by doing all the observations for a single map position at one time relative calibration would be difficult.

Taking these things into account the spectra for the third and fourth quarters were obtained using 320 second integration times and the observing sequence

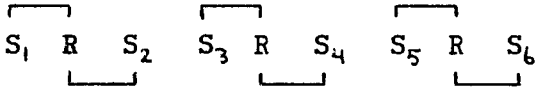


where as before all the $S_1$, $S_2$, $S_3$, ... are different and pairs

$S_i$, $S_j$ using the same R are relatively far apart to minimize the effects of correlated noise. The same map positions, in a different order, would be observed again on other nights.

In table 1 we summarize the dates, positions and observing sequences used to obtain the spectra. Also included is an indication of the atmospheric transparency on each night.

## 2.3 Calibration

The calibration of radio astronomical spectral line observations at millimeter wavelengths is normally a two step process. First, an observed signal intensity is converted to an antenna temperature, $T_A$, by assuming the Rayleigh-Jeans approximation and comparing the observed spectrum to a calibration spectrum of known temperature. In practice this was accomplished by switching off the gain modulator and obtaining a calibration spectrum of the synchronously detected output between the chopper wheel absorber at ambient temperature, $T_{AMB}$, and the sky. The sky temperature, $T_{SKY}$, was measured by comparison to the chart recorder levels of a liquid nitrogen temperature absorber and an ambient temperature absorber placed in front of the feed at the start of the observing session.

TABLE 1

SUMMARY OF OBSERVING PROGRAM

| Date (1978) | Map Positions Observed | Observing Sequence | $\bar{\tau}$ (b) (nepers) |
|---|---|---|---|
| May 19 | first quarter | (S-R) | .45 |
| 20 | | | .42 |
| 21 | | | .33 |
| 25 | | | .40 |
| 30-31 | | | .40 |
| 31-1 | second quarter | R S S R (a) | .39 |
| June 1-2 | | | .38 |
| 2-3 | | | .43 |
| 3-4 | | | .45 |
| 4-5 | R referenced | R R R | .39 |
| 17-18 | third and fourth quarters | S R S | .57 |
| 18-19 | | | .34-.44 |
| 19-20 | | | .42-.50 |
| 20-21 | | | .52-.59 |
| 22-23 | | | .51 |
| 26-27 | poor quality spectra redone | S R S | .55 |
| 27-28 | | | .48 |
| 28-29 | | | .37-.49 |

(a)

Each scan was 640 seconds long for this observing sequence whereas each scan was 320 seconds long for all the other methods.

(b)

This is the atmospheric transparency (see 2.3 Calibration).

The second step is to correct $T_A$ for atmospheric losses ($e^{-\tau_s \sec Z}$) and antenna losses ($\eta$) to determine the true source brightness temperature, $T_A^*$ [1]. The standard result for a plane parallel atmosphere is

$$T_A^* = T_A \, \eta \, e^{-\tau_s \sec z}$$

In the above formula z is the zenith angle of the source and $\tau_s$ is the zenith attenuation in the signal band, which is related to the zenith attenuation in the image band, $\tau_i$, and the average attenuation, $\bar{\tau}$, as follows

$$\bar{\tau} = (\tau_s + \tau_i) / 2$$

Assuming the standard formula

$$T_{SKY} = T_{AMB} (1 - e^{-\bar{\tau} \sec Z})$$

$\bar{\tau}$ can be calculated given the known quantities $T_{SKY}$, $T_{AMB}$ and z. From observation of Orion A and M17 SW, adopting peak brightness temperatures of 70 K and 40 K respectively, we determined that $\tau_s = 1.75 \bar{\tau}$ and $\eta = 0.45$ for CO observations with our 4.75 GHz IF and telescope dish. The equations and brightness temperatures used above can be found in a paper by Ulich and Haas (1976).

---

[1] At millimeter wavelengths this quantity is normally refered to as the excess radiation temperature because it is in fact the excess emission of the line radiation over the continuum radiation of the cosmic background.

## 2.4 Preliminary Processing

After the entire observing program was completed we began to prepare the data for analysis. The first step was to collect and average together all the spectra at the same map position. The average was weighted according to the square of the calibration constant used to convert $T_A$ to $T_A^*$ for each spectrum. Thus

$$\text{Average Spectrum} = \frac{\sum_i C_i^2 \times (\text{ith spectrum})}{\sum_i C_i^2}$$

where

$$C_i = \eta\, e^{-\tau_s \sec z} \Big|_{\text{ith spectrum}}$$

To correct for any CO emission in the reference position, R (3° west of map center), we 'referenced' this position to two other positions, R1 (8° west of map center) and R2 (7.5° west, 2° north of map center). Based on the differences R-R1, R1-R2 and R2-R we adopted the spectrum shown in figure 4 as the CO emission in the reference position. The second step was to add this spectrum to each of the map position average spectra[2].

The third step was to correct the spectrum baselines by removing a second order polynomial fit to those parts of the

---

[2] This is a mistake! The noise profile of figure 4 can be seen in most of the spectra shown in figure 5. All of the reference spectrum except for the region around channel 79 should have been set to zero before adding to the data spectra.

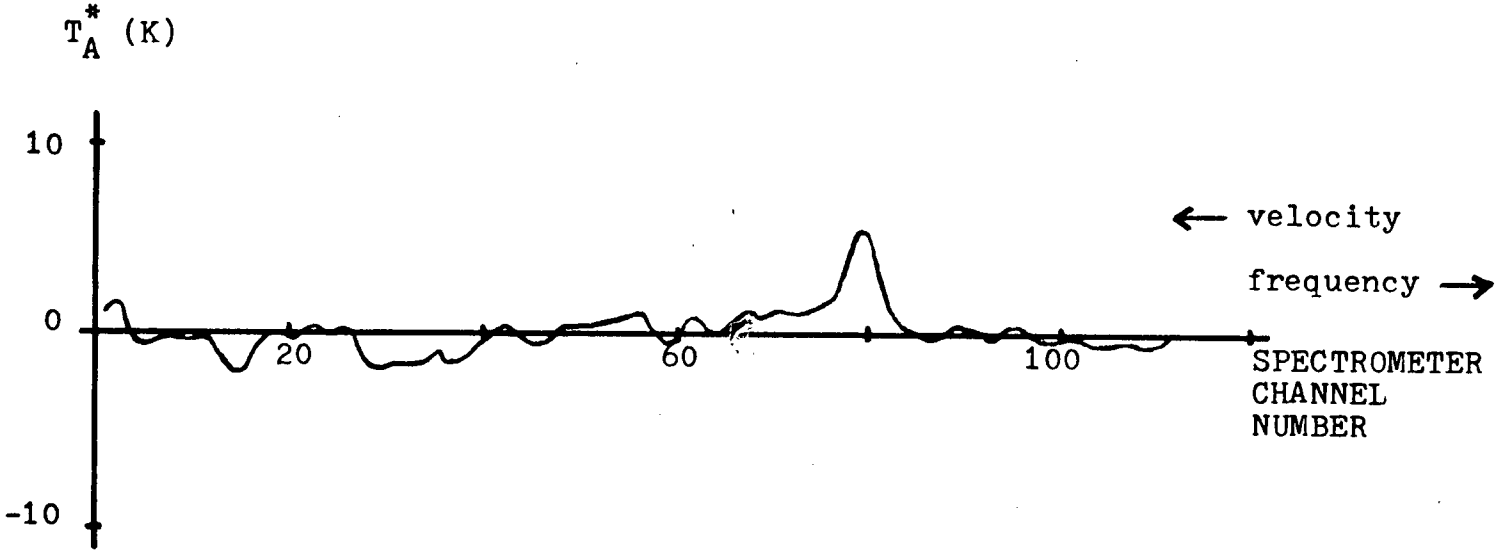


FIGURE 4 : Spectrum at the reference position (located 3 degrees west of map center). The spectrum has been smoothed in frequency by the triangular function described in the text. There is a 5.5K signal peaking in channel number 79 which corresponds to an LSR velocity of 9.3 km/s.

spectrum thought to have no signal (i.e. the first 28 and the last 28 channels). This also allowed us to calculate

$$\sigma = \{ ( \sum_{v=1}^{28} S_v^2 + \sum_{v=85}^{112} S_v^2 ) / 56 \}^{1/2}$$

where v is the channel number and S is the signal in channel v. We adopted $\sigma$ as the root mean square (RMS) deviation for the spectrum.

The final step was to smooth the data to improve the signal to noise ratio. In frequency the data was smoothed by the triangular weighting function

$$S_v \text{ (smoothed)} = ( S_{v-1} + 2 S_v + S_{v+1} ) / 4$$

Spatially the spectra were smoothed by a two dimensional gaussian weighting function of FWHM 0.08 degrees and further weighted by the squares of the RMS deviation $\sigma$ calculated earlier

$$S_v^{\alpha\delta} \text{ (spatially smoothed)} =$$

$$\frac{\sum_{\alpha'\delta'} \sigma_{\alpha'\delta'}^2 \; G[\{(\alpha'-\alpha)^2 + (\delta'-\delta)^2\}^{1/2}] \; S_v^{\alpha'\delta'}}{\sum_{\alpha'\delta'} \sigma_{\alpha'\delta'}^2 \; G[\{(\alpha'-\alpha)^2 + (\delta'-\delta)^2\}^{1/2}]}$$

$$\longrightarrow \quad D(\alpha, \delta, v) = \text{the "observed" data}$$

where the index $\alpha\delta$ refers to the map position of the spectrum and $G(x) = e^{-\alpha x^2}$ ; $G(0.04) = 1/2$.

# 3. DATA ANALYSIS

## 3.1 Representation

Our next problem was to find a meaningful way of displaying the data. We first tried contour plots at fixed velocities. These proved to be difficult to interpret since about 50 of them were required to cover the range of possible velocities. What we needed was a method of compressing our data into a one page 'picture'. We attempted to do this by using color for the velocity dimension and the intensity of the color for the temperature dimension (Allen 1976, Heiles and Jenkins 1976). Since the UBC Computing Center did not have the color graphics facilities required, we devised a process using black and white calcomp plots and color filters to produce the color pictures. After three months of effort we gave up the color picture making. In short the method failed because the human eye does not allow a simple separation of color and color intensity.

After this we tried several different ordered contour and spectra plots finally deciding on the relatively common format shown in figure 5. Figure 5 shows clearly the quality of our spectra but it is difficult to see how features on different spectra correlate. Contour plots showed this correlation quite clearly but of course only at one velocity. It became apparent that we would never clearly 'see' the CO distribution in our data displays.

FIGURE 5 : Ordered spectra plot of the observed data which has been smoothed to a velocity resolution of 5.2 km/s and an angular resolution of 0.08 deg. The center of each square represents the coordinate observed.

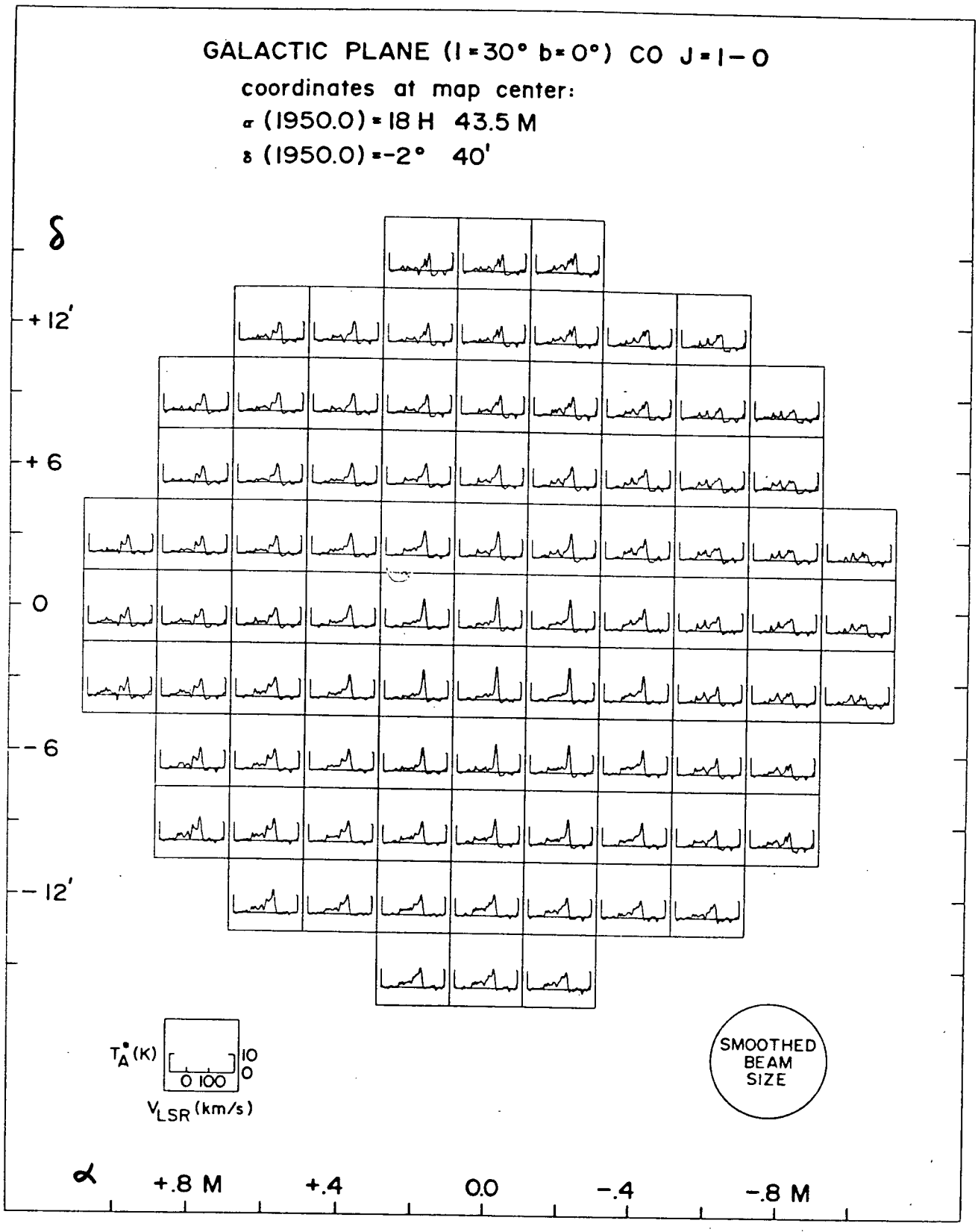
GALACTIC PLANE (l = 30° b = 0°) CO J = 1 – 0
coordinates at map center:
α (1950.0) = 18 H 43.5 M
δ (1950.0) = -2° 40'
δ
+ 12'
+ 6
0
– 6
– 12'
$T_A^*$ (K)
10
0
0 100
$V_{LSR}$ (km/s)
SMOOTHED BEAM SIZE
α
+.8 M
+.4
0.0
–.4
–.8 M

FIGURE 5

## 3.2 Model Fitting

To determine what sort of CO cloud distributions made up our map we did some model fitting. We assumed that a single giant molecular cloud produced a temperature profile given by

$$T(\alpha, \delta, v) = T_o \, e^{- G_s[(\alpha_o-\alpha)^2 + (\delta_o-\delta)^2] - G_f(v_o-v)^2}$$

where $\alpha$, $\delta$ and v are the coordinates in the map and $T_o$, $G_s$, $G_f$, $\alpha_o$, $\delta_o$, $v_o$ are the six parameters which describe the cloud. The simplifying assumption that the temperature due to two clouds $T_i$ and $T_j$ at $(\alpha, \delta, v)$ equals the sum of the individual temperatures

$$T_i(\alpha, \delta, v) + T_j(\alpha, \delta, v)$$

was also made. The model fitting consisted of minimizing

$$E = \sum_{\alpha\delta v} \{ D(\alpha, \delta, v) - \sum_i T_i(\alpha, \delta, v) \}^2$$

with respect to the six parameters $T_o$, $G_s$, $G_f$, $\alpha_o$, $\delta_o$, $v_o$ in each of the $T_i$. This is a nonlinear problem and as far as we know has no general or unique solution.

We proceeded by guessing a solution based on visual inspection of the various plots obtained before. Our initial guess consisted of 12 clouds or 72 parameters for the velocity range 61-113 km/s. We used the Computing Center routine DFNMIN to numerically improve the solution. After a few hundred

iterations two of the clouds disappeared into the noise so we removed them from the solution and continued iterating until convergence with the remaining 10 clouds. The results of this fitting procedure are illustrated in figure 6 and the 6 optimized parameters for each of the 10 clouds are given in table 2. Figure 6(a) shows the data, $D(\alpha, \delta, v)$, and figure 6(b) shows the model, $\sum_i T_i(\alpha, \delta, v)$. The quality of the fit may be judged from the size of the residuals, figure 6(c), which are comparable with the noise in figure 5. For one cloud (cloud 2) quite good estimates of the parameters were obtained from visual inspection of the ordered contour and spectra plots and these did not change significantly from the final values obtained from the fit.

## 3.3 Results

The results of our analysis have been published (Szabo, Shuter and McCutcheon 1980) and can be summarized in the following way. The CO field shows three principal features: (1) an extended feature covering the entire field observed (cloud 1 in table 2) shown in figure 6(d); (2) two 'normal' giant molecular clouds (clouds 2 and 3) shown in figure 6(e) and (f); (3) a blend of 4 clouds with very broad spectral lines all of which have almost the same central velocity (clouds 4,5,6,7) shown in figure 6(g). In addition to the above there are three residual minor clouds (clouds 8,9,10) shown in figure 6(h). We discuss these features in turn.

FIGURE 6 : Plots illustrating the results of model fitting.

a) The observed data, $D(\alpha, \delta, v)$ , between the velocities 61 and 113 km/s in figure 5 is reproduced.

b) The computed spectra found from the sum of the contributions of clouds 1 through 10, $\sum_1 T_i(\alpha, \delta, v)$ .

c) The residuals obtained by subtracting the sum of the contributions in the model (b) from the data (a).

d) The extended feature. This is "cloud" 1 in Table 2.

e&f) The giant molecular clouds 2 and 3 in Table 2.

g) The broad spectral line clouds. This is the sum of the contributions of clouds 4, 5, 6 and 7.

h) The "minor" clouds, so designated because they only contribute 10% to the total integrated CO, whereas the extended feature, the giant molecular clouds and the broad spectral line clouds each contribute about 30%. This is the sum of the contributions of clouds 8, 9 and 10.

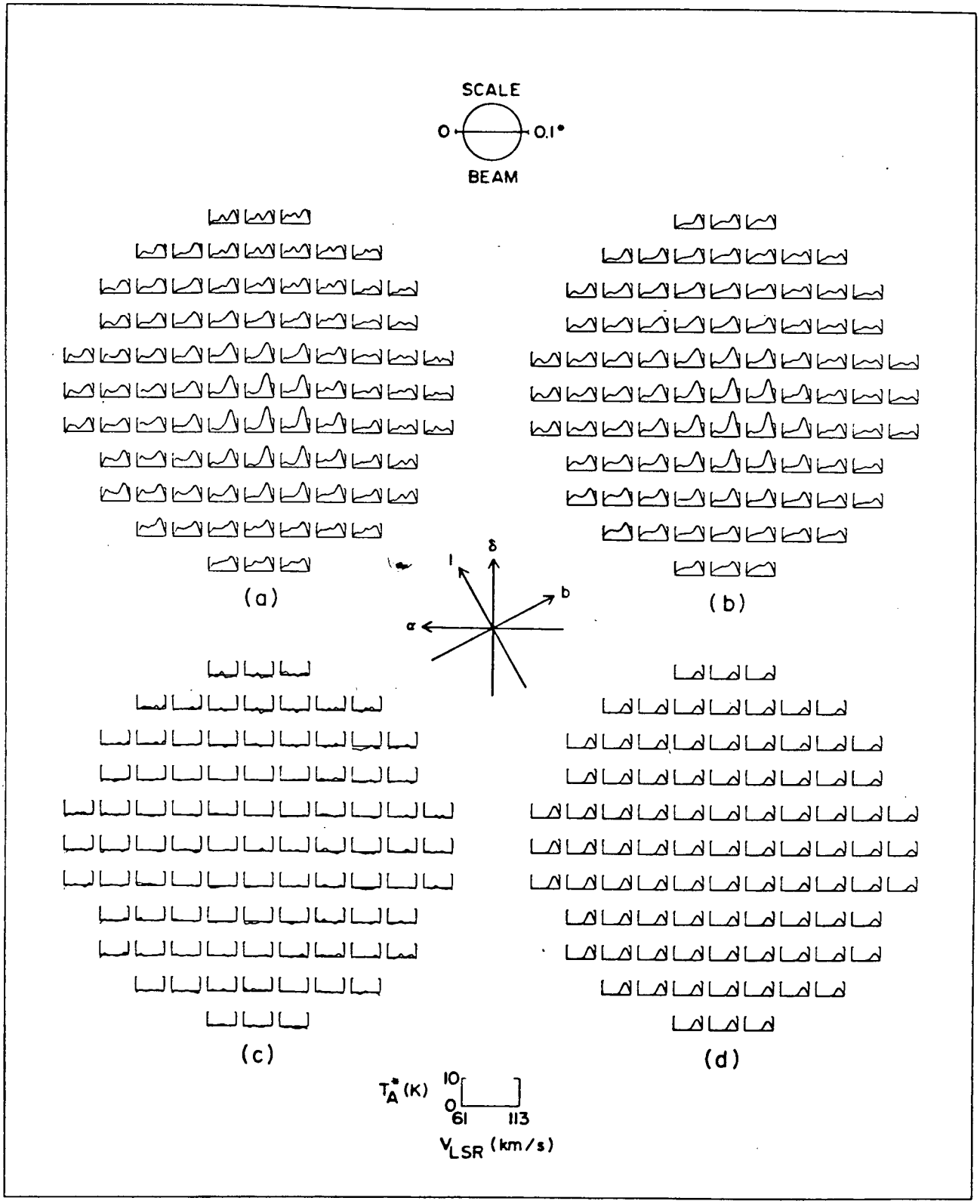


FIGURE 6

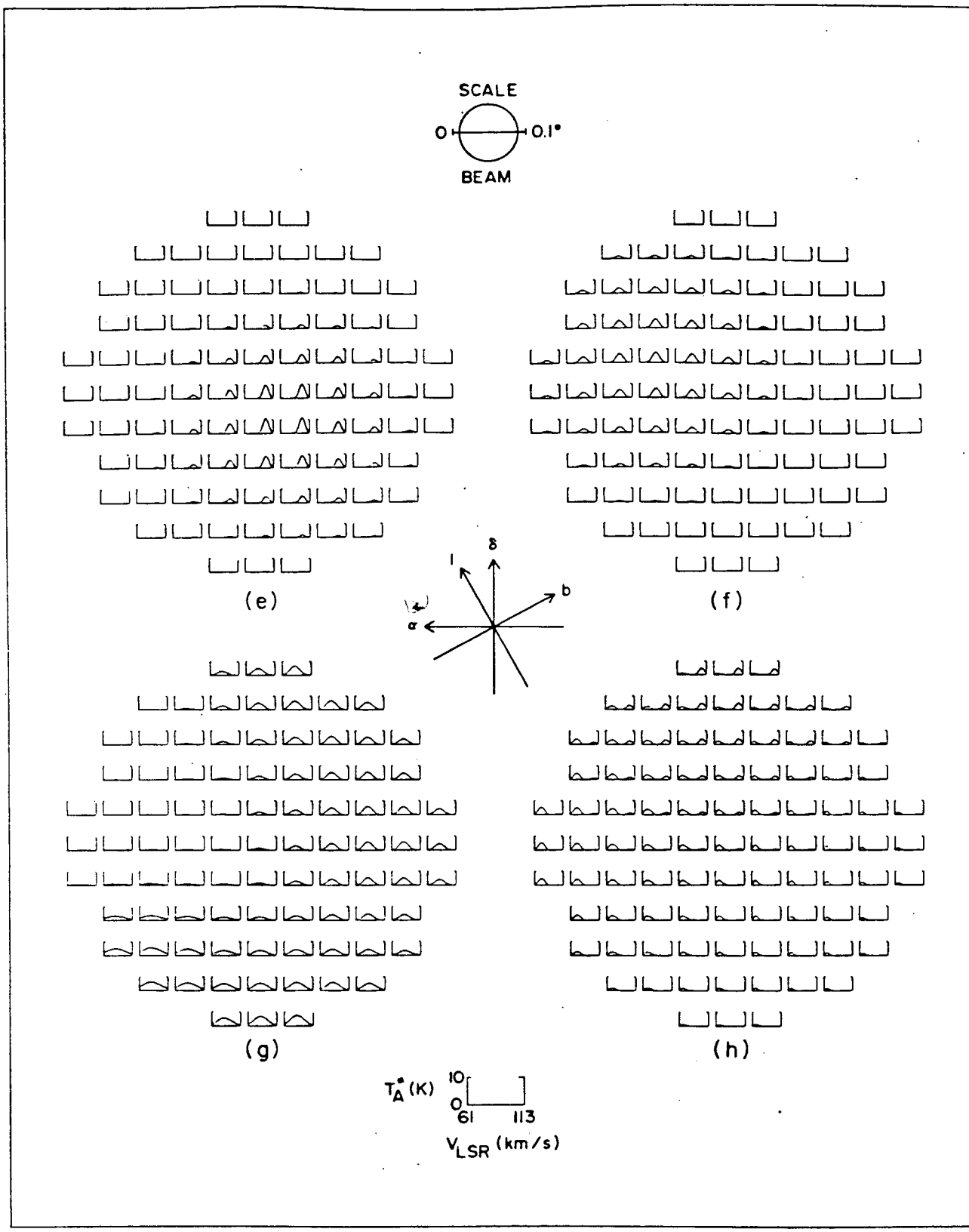


FIGURE 6 cont.

TABLE 2

CLOUD PARAMETERS DERIVED FROM MODEL FITTING

| Cloud | $\Delta\alpha$ (a) (min) | $\Delta\delta$ (arcmin) | Central Velocity (km/s) | Velocity Width FWHM (km/s) | $T_A^*$ (K) | Diameter FWHM (deg) |
|---|---|---|---|---|---|---|
| 1 (b) | - | - | 103.5 | 13.0 | 9.9-3.8 | - |
| 2 | -0.12 | -2.4 | 100.1 | 12.0 | 11.8 | 0.20 |
| 3 | 0.40 | 2.7 | 91.5 | 14.6 | 7.5 | 0.23 |
| 4 | -0.30 | -18.6 | 85.3 | 29.6 | 8.7 | 0.29 |
| 5 | 0.68 | -10.8 | 84.0 | 43.6 | 5.5 | 0.18 |
| 6 | -0.30 | 14.1 | 84.0 | 21.4 | 6.8 | 0.23 |
| 7 | -0.70 | 0.6 | 83.4 | 18.8 | 5.9 | 0.23 |
| 8 | 0.10 | 14.4 | 105.3 | 11.4 | 5.2 | 0.32 |
| 9 | 1.12 | 2.4 | 75.1 | 12.0 | 5.5 | 0.40 |
| 10 | -0.14 | -0.6 | 67.8 | 8.8 | 3.5 | 0.39 |

(a)

These offsets refer to the central coordinate

$\alpha$ (1950) = 18h 43.47m

$\delta$ (1950) = -2° 39.8'

(b)

Extended cloud. The parameters which are not meaningful have been left blank. The temperature increases with decreasing latitude.

(1) The extended feature - figure 6(d):

This feature extends over our entire map, with the temperature increasing in the direction of decreasing galactic latitude. This temperature gradient is perhaps due to the fact that the midplane of the CO distribution is displaced below the conventional plane at this longitude. We have estimated the smoothed out molecular hydrogen number density due to this feature as $n_{H_2}=4$ cm$^{-3}$ (see notes to table 3). Since this feature accounts for about 1/3 of all the CO observed in our field, the total molecular hydrogen number density is in the range $4<n_{H_2}<12$ cm$^{-3}$. Because there must be condensations where $n_{H_2}$ is at least two orders of magnitude higher in order to collisionally excite the $^{12}$CO (Zuckerman and Palmer 1974), it follows that the medium must be clumpy. Thus one interpretation is that there is a clumpy, widespread sheet of CO on the inner edge of the molecular ring, but we cannot tell how far it extends from our limited observations. Using the galactic rotation curve given by Burton and Gordon (1978), the velocity given in table 2 is approximately the tangential velocity at this longitude. This suggests as another interpretation that perhaps this feature is a blend of several clouds around the subcentral point where the radial velocity gradient of the material is a minimum. Johansson, Hjalmarson and Rydbeck (1978) have observed a similar feature in the transition $^2\Pi_{1/2}$, J=1/2 of CH. Their latitude-velocity plot at l=30° shows a feature at ~102 km/s which peaks in intensity at b=-0.25°.

(2) The giant molecular clouds - figure 6(e) and (f):

The distances to these clouds were determined using the rotation curve from Burton and Gordon (1978), and are given in table 3. Because of the ambiguity of distances determined from all velocities except the tangential velocity, both values are given. Also listed in table 3 are the diameters and masses for these two clouds. The range of diameters, 27-42 pc, is in good agreement with values found by Solomon, Sanders and Scoville (1978) but does not agree with those deduced by Burton and Gordon (1978). Notice that the virial mass is in all cases larger than the $^{13}CO$ number density mass. This is another example of the "missing mass" problem which plagues other areas of Astronomy as well. The range of number density masses, (1.5-3.5) x $10^5$ $M_\odot$, agrees well with both observed and predicted values for giant molecular clouds.

(3) The broad spectral line clouds - figure 6(g):

These clouds, with a mean radial velocity of 84 km/s appear to blend to form one irregularly shaped cloud. Their distinguishing feature is their broad linewidths, the average of which is a factor of 2 greater than the average for clouds 2 and 3. Further observations are required to gain insight into the nature and distribution of these broad line clouds.

Our survey has sampled approximately 1/500 of the galactic molecular ring. In this volume we have detected 10 'clouds'. Since most of the 'clouds' in the galaxy are expected to be in the molecular ring, we conclude that there are a total of 5000 'clouds' in the galaxy. (Loosely translate 'clouds' to giant

TABLE 3

ASTROPHYSICAL PARAMETERS FOR CLOUDS 2 AND 3

| Cloud | Distance (kpc) | Diameter (pc) | (a) $N(^{13}CO)$ Mass ($\times 10^5$ $M_\odot$) | (b) Virial Mass ($\times 10^5$ $M_\odot$) |
|---|---|---|---|---|
| 2 | 7.8 | 27 | 2.2 | 5.7 |
| | 9.3 | 32 | 3.1 | 6.8 |
| 3 | 6.9 | 28 | 1.5 | 8.5 |
| | 10.4 | 42 | 3.5 | 12.9 |

(a)

This is the $^{13}CO$ number density mass. We have assumed that the $^{12}CO$ profile is saturated, $T_A^*(^{12}CO)/T_A^*(^{13}CO) = 3$ and LTE is valid. Also we have assumed $N(H_2) = 4.6 \times 10^5 N(^{13}CO)$ and that the mean molecular weight $\mu = 2.33$. For the details of this calculation see McCutcheon and Gregory (1978).

(b)

This is the virial mass first introduced by Solomon (1979). Assuming the cloud is stable and under no external pressure the virial theorem states that the sum of twice the kinetic energy, $3MV^2$ (V = half velocity width in table 2), plus the potential energy, $-3GM^2/5R$, equals zero. Thus

$$\text{Virial Mass} = 5\ R\ V^2\ /\ G$$

molecular clouds.) This agrees well with Solomon, Sanders and Scoville (1978) who quote the total number of giant molecular clouds as 4000 and is two orders of magnitude smaller from the number given by Burton and Gordon (1978) who derive their number based on an indirect statistical model of their one dimensional under sampled data. The total mass of the 'clouds' in the galactic molecular ring comprises about 1% of the total mass of the galaxy.

## 4. CONCLUSION

Data quality and observing time can be optimized significantly in mapping projects by using the observing sequence

$$\overbrace{S_i \; R \; S_2}^{} \quad \overbrace{S_3 \; R \; S_4}^{} \quad \overbrace{S_5 \; R \; S_6}^{} \; \cdots$$

Relative calibration problems are eliminated by collecting spectra at as many different map positions possible every night, or put another way, any map position spectrum is built up from spectra collected on many different nights. Continuity problems are eliminated by sampling 'between map positions'. What this means is never sample the same map position twice, rather offset the second sample half way to the adjacent map position.

Great care should be taken in the methods used to analyse data. We have found that results can vary widely as a function of the data representation and modelling. Nevertheless we are moderately confident of the following conclusions:

-Ten clouds have been detected in our CO observations of a region 1/2° in diameter implying a total number of 5000 clouds in the galactic molecular ring.

-Two of these clouds are well defined giant molecular clouds with masses of the order of $5 \times 10^5$ $M_\odot$ and diameters of about 30 pc.

-Another 'cloud' in more like a sheet of CO covering the entire field and is perhaps a blend of several clouds around the subcentral point.

-A blend of four clouds have linewidths which are a factor of

two larger than those for the well-defined giant molecular clouds.

We were unable to study the detailed shapes of these clouds, which was one of our initial aims, because of the high degree of intrinsic blending of our data. Further investigations in larger fields and at different longitudes seems desirable. Perhaps observations a degree or so off the galactic plane would delineate the individual clouds better. Observations of the same field in $^{13}CO$ would probably produce better definition of the clouds, would enable their masses to be estimated more accurately, and would probably allow one to decide whether our extended feature is a continuous medium or a blend of clouds.

# Bibliography

Allen, R.J. 1976, Sky and Telescope 52, 334.

Burton, W.B., and Gordon, M.A. 1978, Astron. Astrophys. 63, 7.

Gordon, M.A., and Burton, W.B. May 1979, Scientific American 240, 54.

Heiles, C., and Jenkins, E.B. 1976, Astron. Astrophys. 46, 333.

Mahoney, M.J. 1976, Ph. D. Dissertation, University of British Columbia.

McCutcheon, W.H., and Gregory, P.C. 1978, Lecture notes to Physics 570 (unpublished).

Johansson, L.E.B., Hjalmarson, A., and Rydbeck. O.E.H. 1978, paper presented at the I.A.U. Symposium 84, Large Scale Characteristics of the Galaxy (editor W.B. Burton), College Park, Maryland.

Solomon, P.M. 1979, paper presented at the I.A.U. Symposium 87, Interstellar Molecules (editor B.H. Andrew), Mt. Tremblant, Quebec.

Solomon, P.M., Sanders, D.B., and Scoville, N.Z. 1978, paper presented at the I.A.U. Symposium 84, Large Scale Characteristics of the Galaxy (editor W.B. Burton), College Park, Maryland.

Shuter, W.L.H., and McCutcheon, W.H. 1974, Royal Astron. Soc. Canada Jour. 68, 301.

Szabo, A., Shuter, W.L.H., and McCutcheon, W.H. Jan. 1980, Ap. J.

Ulich, B.L., and Haas, R.W. 1976, Ap. J. Suppl. 30, 247.

Zuckerman, B., and Palmer, P. 1974, Annual Review of Astronomy and Astrophysics (editor G.R. Burbidge), Vol 12, 285.